

Observational evidence for the non-suppression effect of atmospheric chemical modification on the ice nucleation activity of East Asian dust

Jingchuan Chen¹, Zhijun Wu^{1,2*}, Xiangxinyue Meng¹, Cuiqi Zhang¹, Jie Chen^{1†}, Yanting Qiu¹, Li Chen³, Xin Fang¹, Yuanyuan Wang⁴, Yinxiao Zhang⁴, Shiyi Chen¹, Jian Gao⁵, Weijun Li⁴, and Min Hu¹

¹State Key Joint Laboratory of Environmental Simulation and Pollution Control, College of Environmental Sciences and Engineering, Peking University, Beijing 100871, China.

²Collaborative Innovation Center of Atmospheric Environment and Equipment Technology, Nanjing University of Information Science and Technology, Nanjing 210044, China.

³Electron Microscopy Laboratory, School of Physics, Peking University, Beijing 100871, China.

⁴Department of Atmospheric Sciences, School of Earth Sciences, Zhejiang University, Hangzhou 310027, China.

⁵State Key Laboratory of Environmental Criteria and Risk Assessment, Chinese Research Academy of Environmental Sciences, Beijing 100012, China.

[†]now at: Institute for Atmospheric and Climate Science, ETHZ, Zurich, 8092, Switzerland

Corresponding author: Zhijun Wu (zhijunwu@pku.edu.cn)

Key Points:

- First direct observational evidence relating to the effects of atmospheric chemical aging on the ice nucleation of East Asian dust.
- The ice nucleation active site densities of aged supermicron particles are close to or slightly higher compared with normal Asian dust.
- Anthropogenic pollution does not impair the ice nucleation activity of East Asian dust in immersion mode.

Abstract

Mineral dust alters cloud microphysical properties by acting as ice-nucleating particles (INPs). The effects of anthropogenic pollution aging on the ice nucleation activity (INA) of mineral dust are still controversial. Such effects were investigated by verifying the chemical aging of airborne size-resolved Asian dust particles via particle chemistry and morphology analyses and comparing the immersion mode INP properties of aged and normal Asian dust. The INP concentrations and ice nucleation active site densities of chemically aged supermicron dust particles (1.0-10.0 μm) were nearly equal to or slightly higher than those of normal Asian dust, which were 0.70-2.45 times and 0.64-4.34 times at -18 °C, respectively. These results reveal that anthropogenic pollution does not notably change the INP concentrations and does not impair the INA of Asian dust. Our work provides direct observational evidence and clarifies the non-suppression effect of anthropogenic pollution on the INA of airborne East Asian dust.

Plain Language Summary

Airborne mineral dust triggers ice formation in clouds by acting as ice-nucleating particles (INPs), potentially influencing weather and climate at regional and global scales. Anthropogenic pollution would modify natural mineral dust during the atmospheric transport process. However, the effects of anthropogenic pollution on the ice nucleation activity of mineral dust remain not well-understood. In this study, we investigated the ice nucleation properties and particle chemical characterizations of collected size-resolved Asian dust samples, and testified the chemical modification of aged dust particles according to the mass concentrations of particulate matter, the water-soluble ion concentrations, the metal element concentrations, and single-particle morphology. The INP concentrations and nucleation activities of aged supermicron Asian dust (1.0 to 10.0 μm) were similar to or slightly higher than those of normal Asian dust, but the difference was not statistically significant. Therefore, anthropogenic pollution does not notably change the INP concentrations and does not impair the ice nucleation activity of Asian dust. This study provides direct observation of naturally aged mineral dust to evaluate the comprehensive effect of anthropogenic pollution on the ice nucleation activity of Asian dust, advancing the understanding of the ice nucleation of airborne aged mineral dust.

1 Introduction

Heterogeneous ice nucleation is a key process in mixed-phase clouds, influencing the water partitioning between ice and liquid phase, and further determining the lifetime, radiative forcing, and precipitation of clouds (Lohmann et al., 2016; Murray et al., 2012). Mineral dust is one of the most important sources of ice-nucleating particles (INPs) due to its high atmospheric loading (Textor et al., 2006), efficient ice nucleation activity (INA) (Hoose & Mohler, 2012), and long-range and even global transport capacity (Pratt et al., 2009; Uno et al., 2009). During the long-range transport, dust particles may mix, adsorb, coagulate or react with other substances (such as biological materials, anthropogenic emissions, and secondary products), and these coatings or reactants may in turn alter the INA of mineral dust (Kanji et al., 2017), affecting cloud formation and their microphysical properties.

Satellite observations and model simulations reported that a considerable fraction of anthropogenic pollutants can act as INPs to catalyze ice formation in clouds (B. Zhao et al., 2019). However, recent studies have found that anthropogenic pollution, particularly black carbon (BC), does not significantly influence regional, global and historical INP concentrations (N_{INP}) relevant to mixed-phase clouds (J. Chen et al., 2018b; Hartmann et al., 2019; Schill et al., 2020). These studies answer the question of anthropogenic contributions to N_{INP} to some extent, but the understanding of effects of anthropogenic activities on the INA of natural INPs such as mineral dust remains to be clarified.

72 Previous laboratory studies have evaluated the effects of various reactants/coatings on the
73 freezing activities of dust INPs. Although the same substance would have different aging effects
74 among different studies due to their experimental design, reaction conditions, and mineral types,
75 most immersion freezing studies agreed that not all inorganic acids reduced the INA of dust
76 particles as H_2SO_4 did (Cziczo et al., 2009; Niedermeier et al., 2010; Sullivan et al., 2010b); the
77 exposure to HNO_3 suggested no distinct impact (Kulkarni et al., 2015; Sullivan et al., 2010a);
78 organic coatings (e.g., levoglucosan) also had an unobservable impact (Kanji et al., 2019; Tobo et
79 al., 2012; Wex et al., 2014); and NH_4^+ and K^+ enhanced the INA of dust (Whale et al., 2018;
80 Worthly et al., 2021; Yun et al., 2020). These deactivation, equivalence, or enhancement effects
81 of varying substances on mineral dust would coexist in the real atmosphere and finally result in a
82 combined effect. Therefore, the actual effect of atmospheric aging on mineral dust, a
83 comprehensive result of multi-species and complex mechanisms, may differ from laboratory
84 aging experiments based on a single substance. In model simulations, the coating effect may
85 obviously alter the INA of particles according to different assumptions (Kulkarni et al., 2015; J.
86 L. Zhu & Penner, 2020), further influencing ice formation in clouds and consequent climate
87 effect. However, the field observation relating to the ice nucleation of mineral dust aged in a real
88 atmosphere is very scarce, which limits the verification of laboratory results and the updating of
89 parameterized schemes in model simulations.

90 Asian dust is the second largest source of dust INPs in the world, and can more efficiently trigger
91 ice nucleation in mixed-phase clouds (Froyd et al., 2022; Kawai et al., 2021). In the downwind
92 of East Asian dust transport path, the severe anthropogenic air pollution occasionally occurred in
93 North China could chemically and/or physically modify these dust particles (Huang et al., 2010;
94 Wu et al., 2020), thus changing the ice nucleation properties of Asian dust. In this study, airborne
95 mineral dust samples were collected during Asian dust events and aged dust periods, respectively.
96 The chemical modification of aged Asian dust particles was confirmed by multiple lines of
97 experimental evidence. On this basis, we compared the INP concentrations and activities of aged
98 and normal Asian dust from the overall and size-resolved perspectives. This study provides
99 direct observation evidence to evaluate the comprehensive effect of anthropogenic pollution on
100 the INA of Asian dust, advancing the understanding of the ice nucleation of airborne aged
101 mineral dust.

2 Materials and Methods

2.1 Sample collection

The samples were collected at the Peking University Atmosphere Environment Monitoring Station (39.99 N, 116.31 E) during the Asian dust events in the spring of 2018 and 2019. An eight-stage Micro-Orifice Deposit Impactor (MOUDI, model 100-R, MSP Corporation, USA) with aerodynamic cut-off diameter (D_{50}) ranging from 0.18 to 10 μm at a flow rate of 30 L min^{-1} (Marple et al., 1991) was applied with polycarbonate filters (47 mm Nuclepore, 0.2 μm pores, Whatman) to collect size-resolved aerosol samples during the Asian dust events, which were forecasted and monitored by China Meteorological Administration (Text S1).

2.2 INP measurements and calculations

As described in J. C. Chen et al. (2021), the sampled filter of each MOUDI stage was extracted by an ultrasonic shaker in 20 mL double-distilled water (resistivity of 18.2 $\text{M}\Omega\text{ cm}$ at 25 $^{\circ}\text{C}$) for 30 min to shake the particles off the filter. Thus, suspended samples containing mineral dust particles were obtained for further INP measurements and chemical analyses.

The PeKing University Ice Nucleation Array (PKUINA), a cold-stage-based instrument, was employed to perform immersion freezing measurements (J. Chen et al., 2018a). Briefly, 90 droplets (1 μL) of suspensions were pipetted onto a hydrophobic glass slide located on the cold stage in each experiment. These droplets were separated from each other by a spacer block and upper and lower glass slides to prevent the Wegener-Bergeron-Findeisen process. A charge-coupled device was employed to monitor the cooling process (cooling rate 1 $^{\circ}\text{C min}^{-1}$) of the cold stage (one frame every 6 s) until all 90 droplets were frozen.

The cumulative number concentration of INP (N_{INP}) per unit volume of sampled air (Vali, 1971) is calculated as:

$$N_{\text{INP}}(T) = \frac{-\ln(1 - f_{\text{ice}}(T))}{V_{\text{air}}} (\text{L}^{-1} \text{ air}) \quad (1)$$

where $f_{\text{ice}}(T)$ is the fraction of frozen droplets in the total 90 droplets above temperature T , and V_{air} is the total volume of sampled air per droplet (standard conditions, 0 $^{\circ}\text{C}$, 1013 hPa) during each sampling period.

As a comparable parameter of INA commonly used for mineral dust, the cumulative ice nucleation active site density n_s (Connolly et al., 2009; Niemand et al., 2012), i.e., the number of active sites per unit surface area of INPs (Vali et al., 2015) is derived from the N_{INP} as:

$$n_s(T) = \frac{N_{INP}(T)}{A} \text{ (m}^{-2}\text{)} \quad (2)$$

where A is the total surface area of particles derived from the online particle number-size distribution measurements within a unit volume of sampled air (aerodynamic diameter, spherical particle hypothesis, 0 °C, 1013 hPa).

Note that, in this study, $N_{INP}(T)$ and $n_s(T)$ for each particle size class (referred to as $N_{INP}(T)$ and $n_s(T)$) and all particle size spectrum (0.18-10 μm , referred to as total $N_{INP}(T)$ and total $n_s(T)$) were calculated. The total $N_{INP}(T)$ is a sum of size-resolved $N_{INP}(T)$ ranging from 0.18 to 10 μm during each dust event. Whereas, the total $n_s(T)$ is the value of total $N_{INP}(T)$ divided by the total surface area of particles in all size classes.

2.3 Particulate matter measurements and chemical analysis

The mass concentrations of particulate matter $\leq 2.5 \mu\text{m}$ ($\text{PM}_{2.5}$) and $10 \mu\text{m}$ (PM_{10}), the BC mass concentration, and the number-size distributions of particulate matter were measured throughout the sampling periods by TH2000Z1 (Text S2), Multi-Angle Absorption Photometer (MAAP, Text S3), and Scanning Mobility Particle Sizers (SMPS, Text S4) coupled with Aerodynamic Particle Sizer (APS, Text S4), respectively. The time resolution for TH2000Z1 was 1 min, and for MAAP, SMPS, and APS was 5 min.

Water-soluble ions and elemental composition in the extracted Asian dust samples (suspensions) were analyzed. For water-soluble inorganic ions (Na^+ , Mg^{2+} , K^+ , Ca^{2+} , NH_4^+ , NO_3^- , SO_4^{2-} , and Cl^-), the suspension was firstly filtered by Polyethersulfone (PES) membrane filters (0.45 μm), and then it was detected by Ion Chromatography (IC, DIONEX ICS-2000/Integrion, Text S5). As for elemental composition (Al, K, Mn, Mg, Ca, Cu, Pb, and Zn), the suspensions containing particles underwent pretreatments until all particles were digested, and then they were determined by the Inductively Coupled Plasma Mass Spectrometry (ICP-MS, XSeries 2, Text S6).

3 Results and Discussion

3.1 Observational evidence of chemically modified Asian dust particles

The collected samples were categorized as aged Asian dust (AAD hereafter, three samples including M8, D2, and D5) and Asian dust (AD hereafter, nine samples including M2, M3, M5, M6, M7, D3, D4, D6, and D7) based on the particle number-size distributions and mass

concentrations, gaseous pollutants, and meteorological parameters during the sampling periods (Figure S1, S2, Table S1, and Text S7). On average, PM_{10} concentrations of the AD and AAD samples were 227.2 ± 123.9 and $203.9 \pm 47.5 \mu g m^{-3}$, respectively, suggesting similar atmospheric dust mass loading. Whereas, the concentrations of $PM_{2.5}$ and BC in AAD were more than twice as high as those in AD (103.7 ± 25.4 vs $43.3 \pm 17.7 \mu g m^{-3}$ for $PM_{2.5}$ and 2.90 ± 0.37 vs $1.33 \pm 0.64 \mu g m^{-3}$ for BC). And the ratio of $PM_{2.5}$ to PM_{10} in AAD was 50.8%, which was much higher than that in AD (19.1%), indicating that there were much more anthropogenic pollutants mixed with dust particles during the AAD periods.

Previous studies have already shown that chemical aging processes enhanced the water-soluble ions by heterogeneous reactions and/or coagulation of $CaCO_3$ with acidic gases (e.g. NO_2 , HNO_3 , SO_2 , and H_2SO_4) and secondary aerosols (e.g. NH_4NO_3 and $(NH_4)_2SO_4$) (Fairlie et al., 2010; Laskin et al., 2005; Underwood et al., 2001; T. Zhu et al., 2011). The mineral composition $CaCO_3$ (~5-30%) was converted to more water-soluble $Ca(NO_3)_2$ or $CaSO_4$ during transport (McNaughton et al., 2009). In the aqueous layer facilitated by $Ca(NO_3)_2$, $CaSO_4$ and NH_4^+ can rapidly form by the coagulation of particulate $(NH_4)_2SO_4$ with dust (Heim et al., 2020). Moreover, NH_4NO_3 can efficiently form on the surface of saline mineral particles (Wu et al., 2020). Therefore, we propose to use the fraction of water-soluble ion in corresponding elemental concentration (f_{wsice}), that is, the ratio of water-soluble ion concentration to corresponding element concentration in the sample, to evaluate the degree of chemical modification of dust particles.

As illustrated in Figure 1 (a) and Table S2, the mean f_{wsice} values of four mental elements (Na, Mg, K, and Ca) were much higher in AAD, especially for Ca, which increased by 67.0% to $90.9 \pm 6.3\%$ compared with AD ($54.4 \pm 10.3\%$). Moreover, size-resolved water-soluble ion analysis revealed that the mean relative mass proportions of Ca^{2+} in supermicron AAD particles ($1.0 \mu m < D_p \leq 10 \mu m$) were higher (3.5-11.2%) than those in AD (Figure 1 (b) and Table S3). Combined with the higher relative mass proportions of NO_3^- (4.8-18.5%, Figure S3 and Table S3), the significant increase of Ca^{2+} in supermicron particles demonstrated the formation of heterogeneous reaction product $Ca(NO_3)_2$ and the more pronounced chemical aging of AAD.

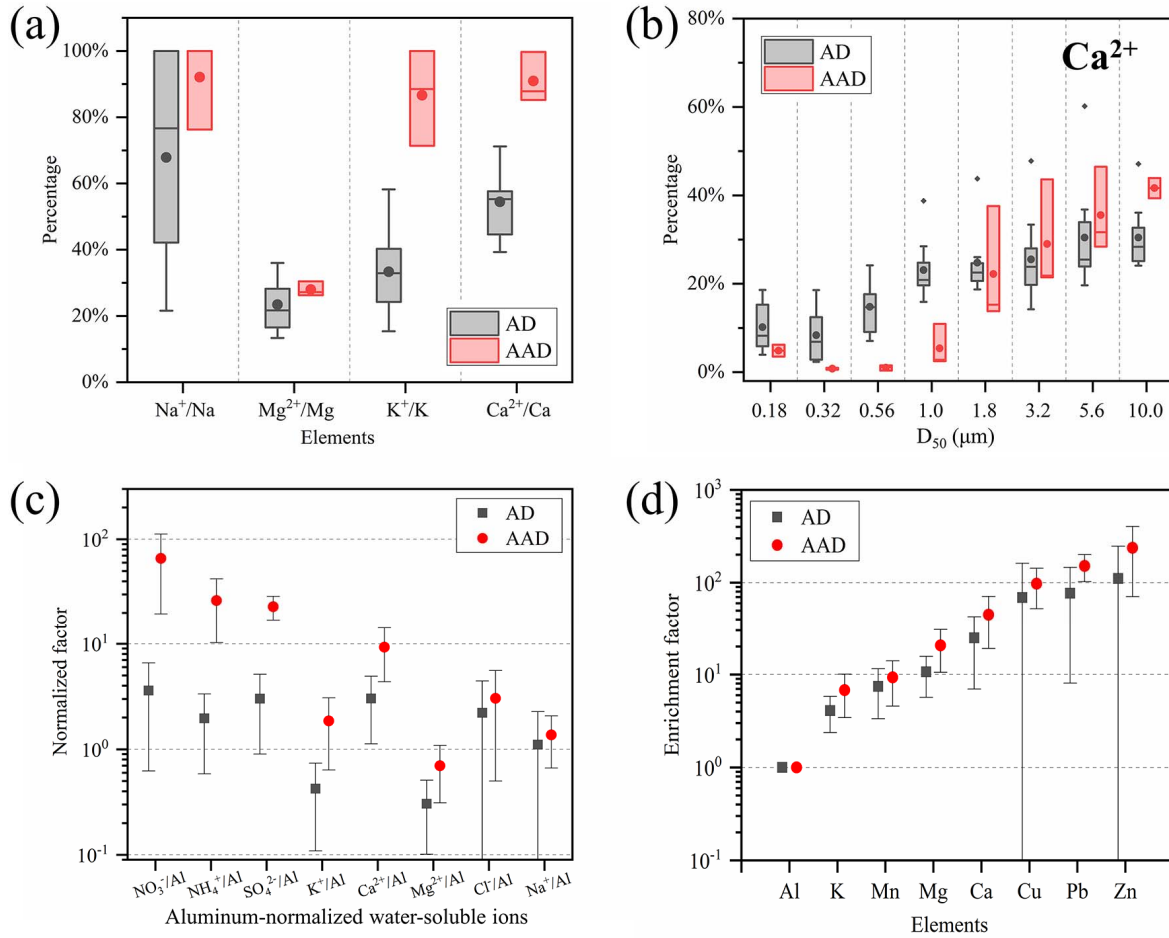


Figure 1. Chemical modification analyses of AD and AAD samples. (a) Fractions of water-soluble ion in corresponding elemental concentration (f_{wsice}) were derived from their IC and ICP-MS measurements. (b) Relative mass proportions of water-soluble calcium ions (Ca^{2+}) in size-resolved AD and AAD samples. (c) Aluminum-normalized water-soluble ions (AWSIs) were the ratio of the concentrations of water-soluble ions to the concentration of reference element Al in the samples. (d) Enrichment factors were derived from the elemental concentrations of aerosol and crust with the reference element Al. Nine AD samples and three AAD samples were analyzed, and they are colored by gray and red, respectively. In the box plot (a) and (b), The boxes represent the interquartile range (IQR, $IQR = Q3 - Q1$). The whiskers represent the range within $1.5 * IQR$. The solid lines, solid circles, and solid diamonds represent the median, mean, and outlier, respectively. Values greater than $Q3 + (1.5 * IQR)$ or less than $Q1 - (1.5 * IQR)$ are defined as outliers. In the scatter plot (c) and (d), AD and AAD are presented as solid gray squares and solid red circles, respectively. Error bars are the standard deviations.

We also calculated the aluminum-normalized water-soluble ions (AWSIs) to quantify the degree of particle aging. Aluminum is a major crustal conservative element with constancy and is often used as a reference element for dust particles (Lawson & Winchester, 1979). Thus, the three

anions and five cations were divided by the concentration of Al respectively to obtain the normalized parameters in Figure 1 (c). Compared with AD, the AWSIs of AAD samples were about one order of magnitude (7.6-18.3 times) higher for aluminum-normalized NO_3^- , NH_4^+ , and SO_4^{2-} (sulfate, nitrate, and ammonium ions, SNA); 2.3-4.4 times higher for K^+ , Ca^{2+} , and Mg^{2+} ; and similar (1.2-1.4 times) for Cl^- and Na^+ (Table S4 and S5). The aging products represented by aluminum-normalized SNA and Ca^{2+} were much higher in AAD, which once again proved that AAD samples had undergone more remarkable atmospheric chemical aging.

Enrichment factors (EFs) of eight elements in AD and AAD are illustrated in Figure 1 (d). The EFs were calculated by the normalization of elemental concentrations in aerosol and crust respected to those of a reference element (Barbieri, 2016). In this study, Al was the reference element and the crustal abundance was given by Wei et al. (1991), so that EF was calculated as $\text{EF} = (\text{X}/\text{Al})_{\text{aerosol}} / (\text{X}/\text{Al})_{\text{crust}}$. Average EFs in AD and AAD samples were generally ranging from 1 to 10 for Al, K, and Mn, suggesting the crustal origin; ranging from 10 to 100 for Mg, Ca, and Cu, suggesting both crustal and anthropogenic origin; >100 for Pb and Zn, implying a significant enrichment from anthropogenic origin. The element EFs of AAD were all about twice as much as those of AD, indicating that the dust particles were more affected by anthropogenic activities during the AAD periods.

Environmental scanning electron microscopy (ESEM) and transmission electron microscopy (TEM) analyses (Kiselev et al., 2017; Li et al., 2016) provided detailed information on collected particles (Figure S4, S5, S6, and Text S8), and the particle morphology of modified Asian dust was observed. In an AAD sample, both mineral dust (Figure S7) and anthropogenic pollutants (soot, i.e., BC, Figure S8) were present, and minerals, soot, organics, and inorganics were internally mixed (Figure S9 and S10), meaning that dust particles were aged by physical adsorption and/or chemical reactions during the AAD periods. Similar results were also reported in previous studies. Li and Shao (2009) found that visible coatings (mainly nitrates) were on the surface of most mineral particles (~90%) during brown haze in Beijing, and up to 32% of dust particles were coated with $\text{Ca}(\text{NO}_3)_2$ in Asian outflow (Li et al., 2014).

In conclusion, we demonstrated that the AAD samples have been significantly aged in the anthropogenic polluted atmosphere. By contrast, the chemical aging degree of AD was notably lower than that of AAD. Based on the aging differences between AD and AAD, the influence of

anthropogenic pollution on the ice nucleation properties of Asian dust would be investigated in the following sections.

3.2 Effects of anthropogenic pollution on the ice nucleation of Asian dust

Figure 2 (a) presents the total N_{INP} of AD and AAD samples, which were 0.47 ± 0.34 and $0.52 \pm 0.42 \text{ L}^{-1}$ at $-10 \text{ }^{\circ}\text{C}$, 2.63 ± 2.04 and $2.99 \pm 2.15 \text{ L}^{-1}$ at $-15 \text{ }^{\circ}\text{C}$, and 3.75 ± 2.90 and $4.41 \pm 2.75 \text{ L}^{-1}$ at $-16 \text{ }^{\circ}\text{C}$ (Table S6), respectively. Although the AAD particles were modified by anthropogenic pollutants, they were in the same INP concentration range (1.11-1.18 times for mean total N_{INP}) as AD samples at -10 , -15 , and $-16 \text{ }^{\circ}\text{C}$. There was no statistically significant difference between the total N_{INP} of AD and AAD (Two-Sample Independent t-Test, $p > 0.05$, Text S9), demonstrating that anthropogenic pollution did not increase or decrease the N_{INP} of natural dust particles. This conclusion is consistent with previous studies showing that anthropogenic pollution has not affected N_{INP} (J. Chen et al., 2018b; Hartmann et al., 2019).

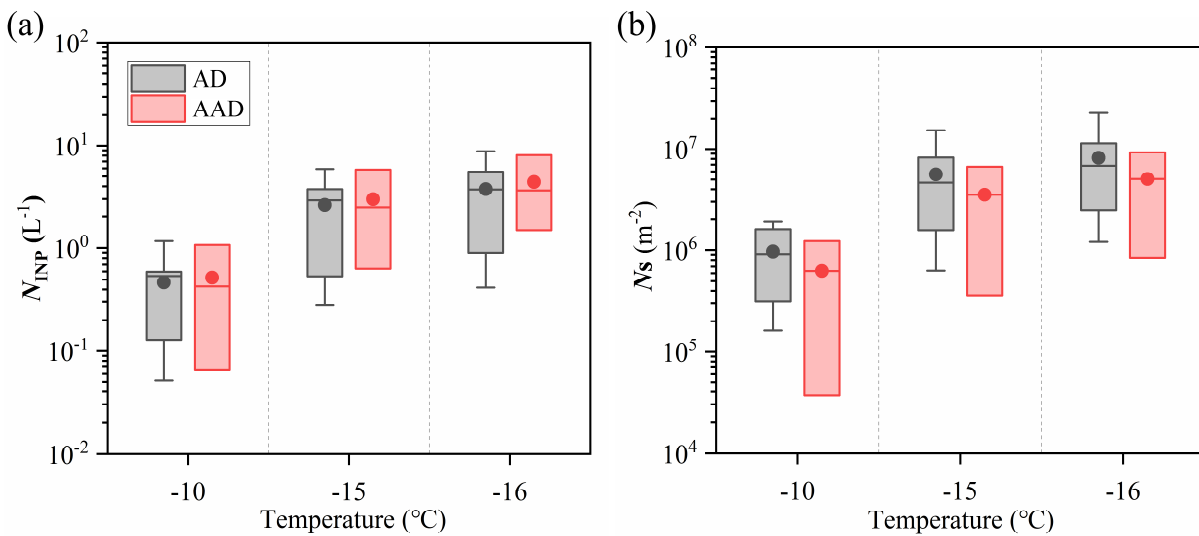


Figure 2. Effects of anthropogenic pollution on the INP concentrations and activities of AD and AAD samples. (a) Total INP concentrations (total N_{INP}) and (b) total ice nucleation active site density (total $n_s(T)$) of AD and AAD samples at three temperatures are colored by gray and red, respectively. Nine AD samples and three AAD samples were involved in the analysis and displayed in box plot. The boxes represent the interquartile range (IQR, $\text{IQR} = Q3 - Q1$). The whiskers represent the range within $1.5 \times \text{IQR}$. The solid lines and solid circles represent the median and mean, respectively.

As depicted in Figure 2 (b), the mean total $n_s(T)$ of AAD samples at three temperatures were slightly lower (0.62-0.65 times) than those of AD samples (Table S6), while the lower quartile

(such as at -10 °C) was up to an order of magnitude lower. Compared with AD, there were more non-dust particles (e.g. urban pollution aerosols) in the submicron AAD ($D_p < 1.0 \mu\text{m}$). These submicron anthropogenic particles contributed less to total N_{INP} than high-activity dust, but had a much higher particle surface area (Figure S11), resulting in a lower total $n_s(T)$ for AAD. Therefore, the actual effects of anthropogenic pollution on the INA of Asian dust need to be further investigated from a size-resolved perspective.

3.3 Aging effects on the ice nucleation of size-resolved Asian dust

The effects of anthropogenic pollution on the INP concentrations and activities of size-resolved particles at -15 and -18 °C are depicted in Figure 3 (a)-(d). Compared with AD, the N_{INP} of AAD were an order of magnitude lower for $D_{50} = 0.18$ and $0.32 \mu\text{m}$; consistent for $D_{50} \geq 0.56 \mu\text{m}$ (such as 0.70-2.45 times at -18 °C, Table S7). Similarly, for particles with $D_{50} < 1.0 \mu\text{m}$, the $n_s(T)$ of AAD samples were 1 to 2 orders of magnitude lower than those of AD, while aged dust was nearly equal to or even more active than AD for $D_{50} \geq 1.0 \mu\text{m}$ at given temperatures (e.g. 0.64-4.34 times at -18 °C). There was a more pronounced size-dependent freezing ability in AAD samples, spanning 5 orders of magnitude, implying that different types of INPs may be included. Combined with the much lower N_{INP} of submicron AAD, we think these much less active submicron INPs were more likely to be anthropogenic pollutant particles in urban areas. That is, AAD samples were mainly composed of submicron urban pollution particles and significantly aged supermicron Asian dust.

To testify above point, we also compared the $n_s(T)$ in this study with urban pollution particles (Pollution-C18 (J. Chen et al., 2018b), marked by dark gray), reference minerals (plagioclase, quartz, albite, and K-feldspar (Harrison et al., 2019), marked by yellow), and dust particles (Asian dust-B19 (Bi et al., 2019), Uncoated AD-K19 (Kanji et al., 2019), and Saharan dust-B16 (Boose et al., 2016), marked by brown) in Figure 3 (d). The $n_s(T)$ of submicron AAD ($D_{50} = 0.18, 0.32, \text{and } 0.56 \mu\text{m}$) were in the same range as Pollution-C18. On the other hand, considering the lower measurement temperatures (-20/-25 °C) in literature studies, the supermicron particles for both AD and AAD samples in this study presented comparable INA with Asian dust-B19 ($D_{50} = 2.5 \mu\text{m}$), Uncoated AD-K19 ($0.01\text{-}3 \mu\text{m}$), Saharan dust-B16 ($D_{50} = 3.5 \mu\text{m}$), and K-feldspar, which were more active than many minerals such as albite,

plagioclase, and quartz, demonstrating that these supermicron particles in AD and AAD were authentic mineral dust.

For supermicron dust particles, the AAD presented similar or slightly higher nucleation activity than AD, but the difference was not statistically significant ($p > 0.05$). In other words, the INA of Asian dust did not decrease after atmospheric aging. This conclusion was supported by Kanji et al. (2019), who found that there was no systematic difference between SOA-coated and uncoated Asian dust (Uncoated AD-K19 and SOA-coated AD-K19 in Figure 3 (d), Table S8, and S9). Similarly, Boose et al. (2016) reported a small positive effect of anthropogenic emissions on the Sahara dust. Based on lidar measurements, He et al. (2021) also revealed that, after long-range transport, the INA of Asian dust mixed with pollutants did not distinctly change. Therefore, we conclude that anthropogenic pollution does not impair the INA of airborne Asian dust.

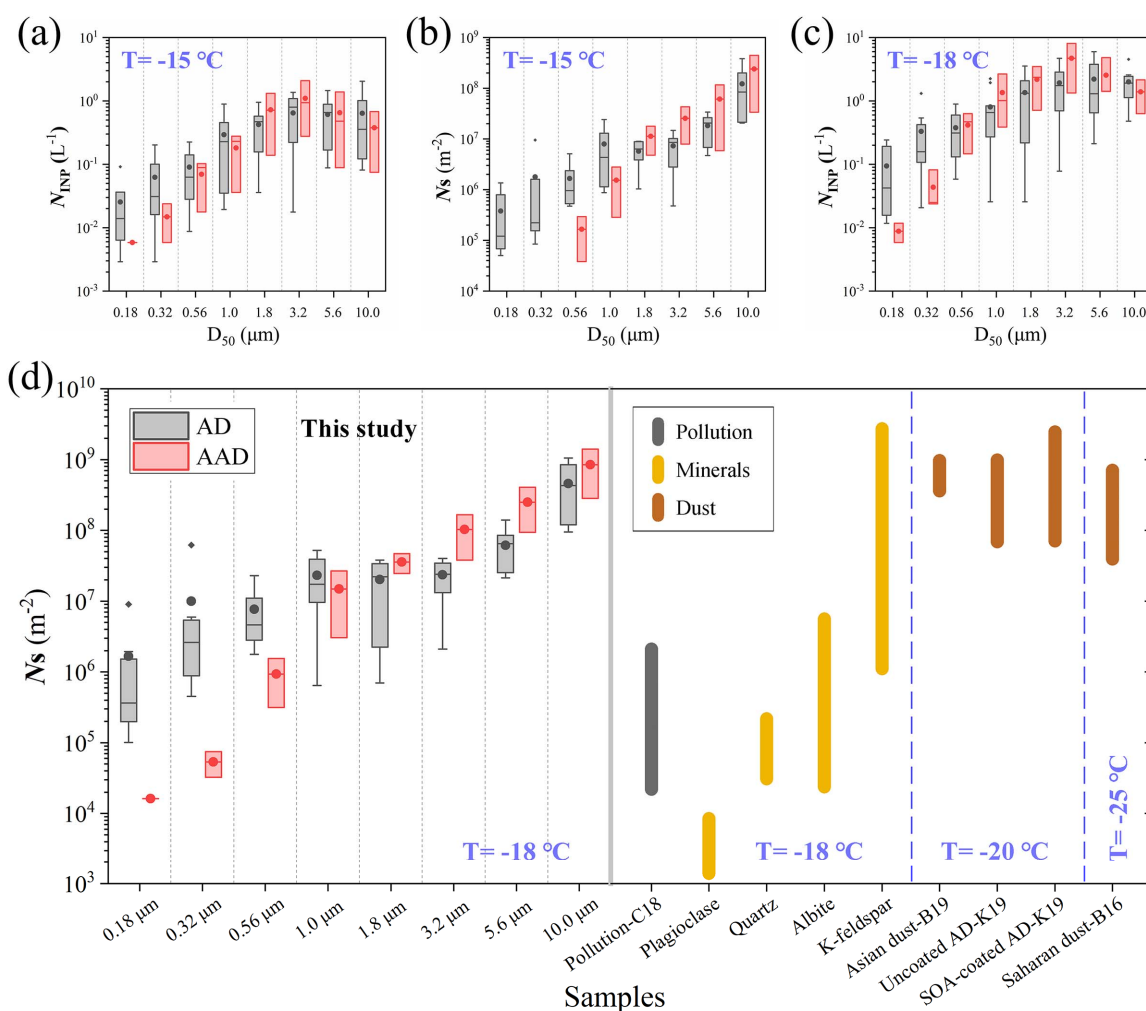


Figure 3. Comparison of the INP concentrations (N_{INP}) and ice nucleation active site densities ($n_s(T)$) among AD, AAD, and literature samples. (a) N_{INP} at -15 °C. (b) $n_s(T)$ at -15 °C. (c) N_{INP} at -18 °C. (d) $n_s(T)$ at -18, -20, and -25 °C. Size-resolved AD and AAD samples in this study are colored by gray and red, respectively, and grouped by particle size classes. The boxes represent the interquartile range (IQR, $IQR = Q3 - Q1$). The whiskers represent the range within $1.5 * IQR$. The solid lines, solid circles, and solid diamonds represent the median, mean, and outlier, respectively. Values greater than $Q3 + (1.5 * IQR)$ or less than $Q1 - (1.5 * IQR)$ are defined as outliers. The $n_s(T)$ of urban pollution particles (Pollution-C18 (J. Chen et al., 2018b), marked by dark gray), reference minerals (Plagioclase, Quartz, Albite, and K-feldspar (Harrison et al., 2019), marked by yellow), and dust particles (Asian dust-B19 (Bi et al., 2019), Uncoated AD-K19 (Kanji et al., 2019), SOA-coated AD-K19 (Kanji et al., 2019), and Saharan dust-B16 (Boose et al., 2016), marked by brown) at -18 °C (or -20/-25 °C) are shown for comparison. Note that the four types of mineral dust particles were summarized by Harrison et al. (2019), and the data were measured in previous studies (Atkinson et al., 2013; Augustin-Bauditz et al., 2014; DeMott et al., 2018; Harrison et al., 2019; Harrison et al., 2016; Losey et al., 2018; Niedermeier et al., 2015; O'Sullivan et al., 2014; Peckhaus et al., 2016; Reicher et al., 2018; Whale et al., 2015; Zolles et al., 2015).

Previous studies have proposed a variety of possible explanations for aging effects based on single substance (e.g. HNO_3 or $(\text{NH}_4)_2\text{SO}_4$) aging experiments. One special aspect of this study is that the dust aging process took place in the atmosphere, thus the observed non-suppression effect of INA by atmospheric aging was a comprehensive reflection of multiple possible reactants and influencing mechanisms. First, alkaline calcite and carbonate might not be good INPs. They could react with acids such as HNO_3 and would move away from the surface of particles in the immersion freezing mode due to the dissolution of water-soluble reaction products in a liquid environment. But new surface-active sites of unreacted particles could be exposed in this process. Second, water-soluble coatings (e.g. NO_3^- and SO_4^{2-}) may not affect the INA of Asian dust. These substances are dissolved and reversibly desorbed from particle surfaces during hygroscopic growth and droplet activation, revealing the concealed active sites and unaffacting freezing (Sullivan et al., 2010a). Third, ion exchange including the suppression of H^+ (Augustin-Bauditz et al., 2014; Kumar et al., 2018; Wex et al., 2014) and the enhancement of NH_4^+/K^+ (Whale et al., 2018; Yun et al., 2020) is likely related to the change of mineral INA. According to the pH-dependent suppression theory from Yun et al. (2021), there is no obvious suppression effect at $\text{pH} > 5$. Mineral dust particles are alkaline and can maintain high pH ($\text{pH} = 5\text{--}7$) in the atmosphere (Pye et al., 2020), especially for the supermicron dust particles (Fang et al., 2017). During the severe air pollution periods in China, the particle pH was also about 4-5 and increased in recent years (Song et al., 2019; Xie et al., 2020). Therefore, the suppression

effect of H^+ on the INA of dust is very limited at the near-neutral particle reaction interface. On the contrary, there is a large amount of NH_4^+ in the ammonia-rich atmosphere of China (Meng et al., 2020; M. Zhao et al., 2016), which may form more active surfaces and enhance the nucleation activity of Asian dust. Finally, the hydrogen bond derived from oxidized hydroxyl groups and adsorbed NH_4^+ could promote ice nucleation on the mineral surface by influencing the orientation of near water molecules (Yakobi-Hancock et al., 2013). To sum up, the little or no effect of carbonate and water-soluble coatings, the unobvious suppression effect of H^+ , and the enhancement effect of NH_4^+/K^+ and hydrogen bond might act together and finally present the non-suppression effect observed in this study.

4 Conclusions

To our knowledge, this work is the first to investigate the influence of anthropogenic pollution on the ice nucleation of airborne mineral dust based on size-resolved Asian dust samples aged in the real atmosphere. The chemical modification of AAD particles was confirmed by combining the air quality conditions during sampling periods, physical and chemical properties of collected particles, and microscopic particle morphology. As the characterization parameters of main products of heterogeneous reactions, the mass fraction of Ca^{2+} in element Ca and the mean relative mass proportions of supermicron Ca^{2+} increased by 67.0% and 3.5-11.2% in AAD particles, respectively. Although the AAD particles have been notably aged by anthropogenic pollution, their total N_{INP} and total $n_s(T)$ were consistent with those of AD particles (0.62-1.18 times) without a statistically significant difference. From a size-resolved perspective, N_{INP} and $n_s(T)$ of supermicron particles for AAD were nearly equal or even slightly higher compared with AD samples (0.64-4.34 times at -18 °C). Thus, we conclude that anthropogenic pollution does not reduce the INP concentrations and INA of Asian dust in the atmosphere.

This study advances the scientific understanding about the effects of anthropogenic pollution on the INA of Asian dust and will contribute to subsequent laboratory studies to further elucidate the combined effect of multi-species association on dust aging. Furthermore, the significant implications of this study are more embodied in the regional and global climatic effects. The dust-driven droplet freezing has been underestimated in model studies (Villanueva et al., 2021). Following previous understanding assuming that the aging process always significantly impairs dust freezing, the bias in simulations of cloud microphysical processes and assessments of radiative effect will further increase under increasing anthropogenic activity scenarios.

Acknowledgments

This work was supported by National Natural Research Foundation of China (NSFC, grant no. 42011530121, 91844301) and Ministry of Science and Technology (MOST, grant no. 2019YFC0214701). We gratefully acknowledge the China Meteorological Administration for the provision of the forecast and monitoring of Asian dust storm and the China National Environmental Monitoring Centre for the air quality monitoring data used in this paper.

Conflict of Interest

The authors declare no conflicts of interest relevant to this study.

Data Availability Statement

The data that support the findings of this study are available at this site (<http://doi.org/10.5281/zenodo.6578828>).

References

- Atkinson, J. D., B. J. Murray, M. T. Woodhouse, T. F. Whale, K. J. Baustian, K. S. Carslaw, et al. (2013). The importance of feldspar for ice nucleation by mineral dust in mixed-phase clouds. *Nature*, 498(7454), 355-358. doi:10.1038/nature12278
- Augustin-Bauditz, S., H. Wex, S. Kanter, M. Ebert, D. Niedermeier, F. Stolz, et al. (2014). The immersion mode ice nucleation behavior of mineral dusts: A comparison of different pure and surface modified dusts. *Geophysical Research Letters*, 41(20), 7375-7382. doi:10.1002/2014gl061317
- Barbieri, M. (2016). The Importance of Enrichment Factor (EF) and Geoaccumulation Index (Igeo) to Evaluate the Soil Contamination. *Journal of Geology & Geophysics*, 5(1). doi:10.4172/2381-8719.1000237
- Bi, K., G. R. McMeeking, D. P. Ding, E. J. T. Levin, P. J. DeMott, D. L. Zhao, et al. (2019). Measurements of Ice Nucleating Particles in Beijing, China. *Journal of Geophysical Research: Atmospheres*, 124(14), 8065-8075. doi:10.1029/2019jd030609
- Boose, Y., B. Sierau, M. I. García, S. Rodríguez, A. Alastuey, C. Linke, et al. (2016). Ice nucleating particles in the Saharan Air Layer. *Atmospheric Chemistry and Physics*, 16(14), 9067-9087. doi:10.5194/acp-16-9067-2016
- Chen, J., X. Y. Pei, H. Wang, J. C. Chen, Y. S. Zhu, M. J. Tang, & Z. J. Wu. (2018a). Development, Characterization, and Validation of a Cold Stage-Based Ice Nucleation Array (PKU-INA). *Atmosphere*, 9(9), 13. doi:10.3390/atmos9090357
- Chen, J., Z. J. Wu, S. Augustin-Bauditz, S. Grawe, M. Hartmann, X. Y. Pei, et al. (2018b). Ice-nucleating particle concentrations unaffected by urban air pollution in Beijing, China. *Atmospheric Chemistry and Physics*, 18(5), 3523-3539. doi:10.5194/acp-18-3523-2018
- Chen, J. C., Z. J. Wu, J. Chen, N. Reicher, X. Fang, Y. Rudich, & M. Hu. (2021). Size-resolved atmospheric ice-nucleating particles during East Asian dust events. *Atmospheric Chemistry and Physics*, 21(5), 3491-3506. doi:10.5194/acp-21-3491-2021
- Connolly, P. J., O. Möhler, P. R. Field, H. Saathoff, R. Burgess, T. Choulaton, & M. Gallagher. (2009). Studies of heterogeneous freezing by three different desert dust samples. *Atmos. Chem. Phys.*, 9(8), 2805-2824. doi:10.5194/acp-9-2805-2009

- Cziczo, D. J., K. D. Froyd, S. J. Gallavardin, O. Moehler, S. Benz, H. Saathoff, & D. M. Murphy. (2009). Deactivation of ice nuclei due to atmospherically relevant surface coatings. *Environmental Research Letters*, 4(4). doi:10.1088/1748-9326/4/4/044013
- DeMott, P. J., O. Möhler, D. J. Cziczo, N. Hiranuma, M. D. Petters, S. S. Petters, et al. (2018). The Fifth International Workshop on Ice Nucleation phase 2 (FIN-02): laboratory intercomparison of ice nucleation measurements. *Atmospheric Measurement Techniques*, 11(11), 6231–6257. doi:10.5194/amt-11-6231-2018
- Fairlie, T. D., D. J. Jacob, J. E. Dibb, B. Alexander, M. A. Avery, A. van Donkelaar, & L. Zhang. (2010). Impact of mineral dust on nitrate, sulfate, and ozone in transpacific Asian pollution plumes. *Atmospheric Chemistry and Physics*, 10(8), 3999–4012. doi:10.5194/acp-10-3999-2010
- Fang, T., H. Guo, L. Zeng, V. Verma, A. Nenes, & R. J. Weber. (2017). Highly Acidic Ambient Particles, Soluble Metals, and Oxidative Potential: A Link between Sulfate and Aerosol Toxicity. *Environmental Science & Technology*, 51(5), 2611–2620. doi:10.1021/acs.est.6b06151
- Froyd, K. D., P. Yu, G. P. Schill, C. A. Brock, A. Kupc, C. J. Williamson, et al. (2022). Dominant role of mineral dust in cirrus cloud formation revealed by global-scale measurements. *Nature Geoscience*. doi:10.1038/s41561-022-00901-w
- Harrison, A. D., K. Lever, A. Sanchez-Marroquin, M. A. Holden, T. F. Whale, M. D. Tarn, et al. (2019). The ice-nucleating ability of quartz immersed in water and its atmospheric importance compared to K-feldspar. *Atmospheric Chemistry and Physics*, 19(17), 11343–11361. doi:10.5194/acp-19-11343-2019
- Harrison, A. D., T. F. Whale, M. A. Carpenter, M. A. Holden, L. Neve, D. O'Sullivan, et al. (2016). Not all feldspars are equal: a survey of ice nucleating properties across the feldspar group of minerals. *Atmospheric Chemistry and Physics*, 16(17), 10927–10940. doi:10.5194/acp-16-10927-2016
- Hartmann, M., T. Blunier, S. O. Brügger, J. Schmale, M. Schwikowski, A. Vogel, et al. (2019). Variation of Ice Nucleating Particles in the European Arctic Over the Last Centuries. *Geophysical Research Letters*, 46(7), 4007–4016. doi:10.1029/2019GL082311
- He, Y., F. Yi, Y. Yi, F. Liu, & Y. Zhang. (2021). Heterogeneous Nucleation of Midlevel Cloud Layer Influenced by Transported Asian Dust Over Wuhan (30.5°N, 114.4°E), China. *Journal of Geophysical Research: Atmospheres*, 126(2). doi:10.1029/2020JD033394
- Heim, E. W., J. Dibb, E. Scheuer, P. C. Jost, B. A. Nault, J. L. Jimenez, et al. (2020). Asian dust observed during KORUS-AQ facilitates the uptake and incorporation of soluble pollutants during transport to South Korea. *Atmospheric Environment*, 224. doi:10.1016/j.atmosenv.2020.117305
- Hoose, C., & O. Mohler. (2012). Heterogeneous ice nucleation on atmospheric aerosols: a review of results from laboratory experiments. *Atmospheric Chemistry and Physics*, 12(20), 9817–9854. doi:10.5194/acp-12-9817-2012
- Huang, K., G. Zhuang, J. Li, Q. Wang, Y. Sun, Y. Lin, & J. S. Fu. (2010). Mixing of Asian dust with pollution aerosol and the transformation of aerosol components during the dust storm over China in spring 2007. *Journal of Geophysical Research*, 115. doi:10.1029/2009JD013145
- Kanji, Z. A., L. Ladino, H. Wex, Y. Boose, M. Burkert-Kohn, D. Cziczo, & M. Krämer. (2017). Ice Formation and Evolution in Clouds and Precipitation: Measurement and Modeling Challenges. Chapter 1: Overview of Ice Nucleating Particles. *Meteorological Monographs*, 58, 1–25. doi:10.1175/AMSMONOGRAPHS-D-0006.1
- Kanji, Z. A., R. C. Sullivan, M. Niemand, P. J. DeMott, A. J. Prenni, C. Chou, et al. (2019). Heterogeneous ice nucleation properties of natural desert dust particles coated with a surrogate of secondary organic aerosol. *Atmospheric Chemistry and Physics*, 19(7), 5091–5110. doi:10.5194/acp-19-5091-2019
- Kawai, K., H. Matsui, & Y. Tobo. (2021). High Potential of Asian Dust to Act as Ice Nucleating Particles in Mixed-Phase Clouds Simulated With a Global Aerosol-Climate Model. *Journal of Geophysical Research: Atmospheres*, 126(12). doi:10.1029/2020jd034263
- Kiselev, A., F. Bachmann, P. Pedevilla, S. J. Cox, A. Michaelides, D. Gerthsen, & T. Leisner. (2017). Active sites in heterogeneous ice nucleation—the example of K-rich feldspars. *Science*, 355(6323), 367–371. doi:10.1126/science.aai8034
- Kulkarni, G., K. Zhang, C. Zhao, M. Nandasiri, V. Shutthanandan, X. Liu, et al. (2015). Ice formation on nitric acid-coated dust particles: Laboratory and modeling studies. *Journal of Geophysical Research: Atmospheres*, 120(15), 7682–7698. doi:10.1002/2014jd022637
- Kumar, A., C. Marcolli, B. Luo, & T. Peter. (2018). Ice nucleation activity of silicates and aluminosilicates in pure water and aqueous solutions – Part 1: The K-feldspar microcline. *Atmospheric Chemistry and Physics*, 18(10), 7057–7079. doi:10.5194/acp-18-7057-2018
- Laskin, A., M. Iedema, A. Ichkovich, E. Graber, I. Taraniuk, & Y. Rudich. (2005). Direct observation of completed processed calcium carbonate dust particles. *Faraday Discussions*, 130, 453–468; discussion 491. doi:10.1039/B417366J

- Lawson, D. R., & J. W. Winchester. (1979). Standard Crustal Aerosol as a Reference for Elemental Enrichment Factors. *Atmospheric Environment*, 13(7), 925-930. doi:10.1016/0004-6981(79)90003-9
- Li, W. J., & L. Y. Shao. (2009). Observation of nitrate coatings on atmospheric mineral dust particles. *Atmos. Chem. Phys.*, 9(6), 1863-1871. doi:10.5194/acp-9-1863-2009
- Li, W. J., L. Y. Shao, Z. B. Shi, J. M. Chen, L. X. Yang, Q. Yuan, et al. (2014). Mixing state and hygroscopicity of dust and haze particles before leaving Asian continent. *Journal of Geophysical Research-Atmospheres*, 119(2), 1044-1059. doi:10.1002/2013jd021003
- Li, W. J., L. Y. Shao, D. Z. Zhang, C. U. Ro, M. Hu, X. H. Bi, et al. (2016). A review of single aerosol particle studies in the atmosphere of East Asia: morphology, mixing state, source, and heterogeneous reactions. *Journal of Cleaner Production*, 112, 1330-1349. doi:10.1016/j.jclepro.2015.04.050
- Lohmann, U., F. Lüönd, & F. Mahrt. (2016). *An Introduction to Clouds: From the Microscale to Climate*. Cambridge: Cambridge University Press.
- Losey, D. J., S. K. Sihvonen, D. P. Veghte, E. Chong, & M. A. Freedman. (2018). Acidic processing of fly ash: chemical characterization, morphology, and immersion freezing. *Environmental Science: Processes & Impacts*, 20(11), 1581-1592. doi:10.1039/C8EM00319J
- Marple, V. A., K. L. Rubow, & S. M. Behm. (1991). A Microorifice Uniform Deposit Impactor (MOUDI): Description, Calibration, and Use. *Aerosol Science and Technology*, 14(4), 434-446. doi:10.1080/02786829108959504
- McNaughton, C. S., A. D. Clarke, V. Kapustin, Y. Shinozuka, S. G. Howell, B. E. Anderson, et al. (2009). Observations of heterogeneous reactions between Asian pollution and mineral dust over the Eastern North Pacific during INTEX-B. *Atmos. Chem. Phys.*, 9(21), 8283-8308. doi:10.5194/acp-9-8283-2009
- Meng, Z., L. Wu, X. Xu, W. Xu, R. Zhang, X. Jia, et al. (2020). Changes in ammonia and its effects on PM2.5 chemical property in three winter seasons in Beijing, China. *Sci Total Environ*, 749, 142208. doi:10.1016/j.scitotenv.2020.142208
- Murray, B. J., D. O'Sullivan, J. D. Atkinson, & M. E. Webb. (2012). Ice nucleation by particles immersed in supercooled cloud droplets. *Chem Soc Rev*, 41(19), 6519-6554. doi:10.1039/c2cs35200a
- Niedermeier, D., S. Augustin-Bauditz, S. Hartmann, H. Wex, K. Ignatius, & F. Stratmann. (2015). Can we define an asymptotic value for the ice active surface site density for heterogeneous ice nucleation? *Journal of Geophysical Research: Atmospheres*, 120(10), 5036-5046. doi:10.1002/2014jd022814
- Niedermeier, D., S. Hartmann, R. A. Shaw, D. Covert, T. F. Mentel, J. Schneider, et al. (2010). Heterogeneous freezing of droplets with immersed mineral dust particles – measurements and parameterization. *Atmos. Chem. Phys.*, 10(8), 3601-3614. doi:10.5194/acp-10-3601-2010
- Niemand, M., O. Möhler, B. Vogel, H. Vogel, C. Hoose, P. Connolly, et al. (2012). A Particle-Surface-Area-Based Parameterization of Immersion Freezing on Desert Dust Particles. *Journal of the Atmospheric Sciences*, 69(10), 3077-3092. doi:10.1175/jas-d-11-0249.1
- O'Sullivan, D., B. J. Murray, T. L. Malkin, T. F. Whale, N. S. Umo, J. D. Atkinson, et al. (2014). Ice nucleation by fertile soil dusts: relative importance of mineral and biogenic components. *Atmos. Chem. Phys.*, 14(4), 1853-1867. doi:10.5194/acp-14-1853-2014
- Peckhaus, A., A. Kiselev, T. Hiron, M. Ebert, & T. Leisner. (2016). A comparative study of K-rich and Na/Ca-rich feldspar ice-nucleating particles in a nanoliter droplet freezing assay. *Atmospheric Chemistry and Physics*, 16(18), 11477-11496. doi:10.5194/acp-16-11477-2016
- Pratt, K. A., P. J. DeMott, J. R. French, Z. Wang, D. L. Westphal, A. J. Heymsfield, et al. (2009). In situ detection of biological particles in cloud ice-crystals. *Nature Geoscience*, 2(6), 398-401. doi:10.1038/ngeo521
- Pye, H. O. T., A. Nenes, B. Alexander, A. P. Ault, M. C. Barth, S. L. Clegg, et al. (2020). The acidity of atmospheric particles and clouds. *Atmos. Chem. Phys.*, 20(8), 4809-4888. doi:10.5194/acp-20-4809-2020
- Reicher, N., L. Segev, & Y. Rudich. (2018). The Weizmann Supercooled Droplets Observation on a Microarray (WISDOM) and application for ambient dust. *Atmospheric Measurement Techniques*, 11(1), 233-248. doi:10.5194/amt-11-233-2018
- Schill, G. P., P. J. DeMott, E. W. Emerson, A. M. C. Rauker, J. K. Kodros, K. J. Suski, et al. (2020). The contribution of black carbon to global ice nucleating particle concentrations relevant to mixed-phase clouds. *Proceedings of the National Academy of Sciences*, 117(37), 22705. doi:10.1073/pnas.2001674117
- Song, S., A. Nenes, M. Gao, Y. Zhang, P. Liu, J. Shao, et al. (2019). Thermodynamic Modeling Suggests Declines in Water Uptake and Acidity of Inorganic Aerosols in Beijing Winter Haze Events during 2014/2015–2018/2019. *Environmental Science & Technology Letters*, 6(12), 752-760. doi:10.1021/acs.estlett.9b00621

- Sullivan, R. C., L. Miñambres, P. J. DeMott, A. J. Prenni, C. M. Carrico, E. J. T. Levin, & S. M. Kreidenweis. (2010a). Chemical processing does not always impair heterogeneous ice nucleation of mineral dust particles. *Geophysical Research Letters*, 37(24), n/a-n/a. doi:10.1029/2010gl045540
- Sullivan, R. C., M. D. Petters, P. J. DeMott, S. M. Kreidenweis, H. Wex, D. Niedermeier, et al. (2010b). Irreversible loss of ice nucleation active sites in mineral dust particles caused by sulphuric acid condensation. *Atmos. Chem. Phys.*, 10(23), 11471-11487. doi:10.5194/acp-10-11471-2010
- Textor, C., M. Schulz, S. Guibert, S. Kinne, Y. Balkanski, S. Bauer, et al. (2006). Analysis and quantification of the diversities of aerosol life cycles within AeroCom. *Atmos. Chem. Phys.*, 6(7), 1777-1813. doi:10.5194/acp-6-1777-2006
- Tobo, Y., P. J. DeMott, M. Raddatz, D. Niedermeier, S. Hartmann, S. M. Kreidenweis, et al. (2012). Impacts of chemical reactivity on ice nucleation of kaolinite particles: A case study of levoglucosan and sulfuric acid. *Geophysical Research Letters*, 39(19), n/a-n/a. doi:10.1029/2012gl053007
- Underwood, G. M., C. H. Song, M. Phadnis, G. R. Carmichael, & V. H. Grassian. (2001). Heterogeneous reactions of NO₂ and HNO₃ on oxides and mineral dust: A combined laboratory and modeling study. *Journal of Geophysical Research: Atmospheres*, 106(D16), 18055-18066. doi:10.1029/2000JD900552
- Uno, I., K. Eguchi, K. Yumimoto, T. Takemura, A. Shimizu, M. Uematsu, et al. (2009). Asian dust transported one full circuit around the globe. *Nature Geoscience*, 2(8), 557-560. doi:10.1038/ngeo583
- Vali, G. (1971). Quantitative evaluation of experimental results on the heterogeneous freezing nucleation of supercooled liquids. *Journal of the Atmospheric Sciences*, 28(3), 402-409.
- Vali, G., P. J. DeMott, O. Möhler, & T. F. Whale. (2015). Technical Note: A proposal for ice nucleation terminology. *Atmos. Chem. Phys.*, 15(18), 10263-10270. doi:10.5194/acp-15-10263-2015
- Villanueva, D., D. Neubauer, B. Gasparini, L. Ickes, & I. Tegen. (2021). Constraining the Impact of Dust-Driven Droplet Freezing on Climate Using Cloud-Top-Phase Observations. *Geophysical Research Letters*, 48(11). doi:10.1029/2021gl092687
- Wei, F., C. Zheng, J. Chen, & Y. Wu. (1991). Study on the Background Contents on 61 Elements of Soils in China. *Environmental Science*, 12(4), 12-19. doi:10.13227/j.hjlx.1991.04.005
- Wex, H., P. J. DeMott, Y. Tobo, S. Hartmann, M. Rösch, T. Clauss, et al. (2014). Kaolinite particles as ice nuclei: learning from the use of different kaolinite samples and different coatings. *Atmos. Chem. Phys.*, 14(11), 5529-5546. doi:10.5194/acp-14-5529-2014
- Whale, T. F., M. A. Holden, T. W. Wilson, D. O'Sullivan, & B. J. Murray. (2018). The enhancement and suppression of immersion mode heterogeneous ice-nucleation by solutes. *Chem Sci*, 9(17), 4142-4151. doi:10.1039/c7sc05421a
- Whale, T. F., B. J. Murray, amp, apos, D. Sullivan, T. W. Wilson, et al. (2015). A technique for quantifying heterogeneous ice nucleation in microlitre supercooled water droplets. *Atmospheric Measurement Techniques*, 8(6), 2437-2447. doi:10.5194/amt-8-2437-2015
- Worthy, S. E., A. Kumar, Y. Xi, J. Yun, J. Chen, C. Xu, et al. (2021). The effect of (NH₄)₂SO₄ on the freezing properties of non-mineral dust ice-nucleating substances of atmospheric relevance. *Atmos. Chem. Phys.*, 21(19), 14631-14648. doi:10.5194/acp-21-14631-2021
- Wu, C., S. Zhang, G. Wang, S. Lv, D. Li, L. Liu, et al. (2020). Efficient Heterogeneous Formation of Ammonium Nitrate on the Saline Mineral Particle Surface in the Atmosphere of East Asia during Dust Storm Periods. *Environ Sci Technol*, 54(24), 15622-15630. doi:10.1021/acs.est.0c04544
- Xie, Y., G. Wang, X. Wang, J. Chen, Y. Chen, G. Tang, et al. (2020). Nitrate-dominated PM_{2.5} and elevation of particle pH observed in urban Beijing during the winter of 2017. *Atmospheric Chemistry and Physics*, 20(8), 5019-5033. doi:10.5194/acp-20-5019-2020
- Yakobi-Hancock, J. D., L. A. Ladino, & J. P. D. Abbatt. (2013). Feldspar minerals as efficient deposition ice nuclei. *Atmospheric Chemistry and Physics*, 13(22), 11175-11185. doi:10.5194/acp-13-11175-2013
- Yun, J., A. Kumar, N. Removski, A. Shchukarev, N. Link, J.-F. Boily, & A. K. Bertram. (2021). Effects of Inorganic Acids and Organic Solutes on the Ice Nucleating Ability and Surface Properties of Potassium-Rich Feldspar. *Acs Earth and Space Chemistry*, 5(5), 1212-1222. doi:10.1021/acsearthspacechem.1c00034
- Yun, J., N. Link, A. Kumar, A. Shchukarev, J. Davidson, A. Lam, et al. (2020). Surface Composition Dependence on the Ice Nucleating Ability of Potassium-Rich Feldspar. *Acs Earth and Space Chemistry*, 4(6), 873-881. doi:10.1021/acsearthspacechem.0c00077
- Zhao, B., Y. Wang, Y. Gu, K.-N. Liou, J. H. Jiang, J. Fan, et al. (2019). Ice nucleation by aerosols from anthropogenic pollution. *Nature Geoscience*, 12(8), 602-607. doi:10.1038/s41561-019-0389-4

- Zhao, M., S. Wang, J. Tan, Y. Hua, D. Wu, & J. Hao. (2016). Variation of Urban Atmospheric Ammonia Pollution and its Relation with PM_{2.5} Chemical Property in Winter of Beijing, China. *Aerosol and Air Quality Research*, 16(6), 1390-1402. doi:10.4209/aaqr.2015.12.0699
- Zhu, J. L., & J. E. Penner. (2020). Radiative forcing of anthropogenic aerosols on cirrus clouds using a hybrid ice nucleation scheme. *Atmospheric Chemistry and Physics*, 20(13), 7801-7827. doi:10.5194/acp-20-7801-2020
- Zhu, T., J. Shang, & D. F. Zhao. (2011). The roles of heterogeneous chemical processes in the formation of an air pollution complex and gray haze. *Science China-Chemistry*, 54(1), 145-153. doi:10.1007/s11426-010-4181-y
- Zolles, T., J. Burkart, T. Hausler, B. Pummer, R. Hitzemberger, & H. Grothe. (2015). Identification of ice nucleation active sites on feldspar dust particles. *J Phys Chem A*, 119(11), 2692-2700. doi:10.1021/jp509839x